Sigma-Nucleus Potential in $A = 28$

H. Noumi,[1] P. K. Saha,[1,*] D. Abe,[2] S. Ajimura,[3] K. Aoki,[1] H. C. Bhang,[4] T. Endo,[2] Y. Fujii,[2] T. Fukuda,[1,*] H. C. Guo,[5] K. Imai,[7] O. Hashimoto,[2] H. Hotchi,[6,†] E. H. Kim,[4] J. H. Kim,[4] T. Kishimoto,[3] A. Krutenkova,[8] K. Maeda,[2] T. Nagae,[1] M. Nakamura,[6] H. Outa,[1] M. Sekimoto,[1] T. Saito,[2,‡] A. Sakaguchi,[3] Y. Sato,[1,2] R. Sawafta,[9] Y. Shimizu,[3,*] T. Takahashi,[2] L. Tang,[10] H. Tamura,[2] K. Tanida,[6] T. Watanabe,[2] H. H. Xia,[5] S. H. Zhou,[5] L. H. Zhu,[7] and X. F. Zhu[5]

[1]*High Energy Accelerator Research Organization (KEK), Tsukuba, Ibaraki 305-0801, Japan*
[2]*Department of Physics, Tohoku University, Sendai 980-8578, Japan*
[3]*Department of Physics, Osaka University, Toyonaka, Osaka 560-0043, Japan*
[4]*Department of Physics, Seoul National University, Seoul 151-742, Korea*
[5]*Department of Nuclear Physics, CIAE, P.O. Box 275(80), Beijing 102413, China*
[6]*Graduate School of Science, University of Tokyo, Tokyo 113-003, Japan*
[7]*Department of Physics, Kyoto University, Sakyo, Kyoto 606-8502, Japan*
[8]*Institute of Theoretical and Experimental Physics, Moscow 117218, Russia*
[9]*Physics Department, North Carolina A&T State University, Greensboro, North Carolina 27411*
[10]*Department of Physics, Hampton University, Hampton, Virginia 23668*

(Received 16 December 2001; published 30 July 2002)

We have studied the (π^-, K^+) reaction on a silicon target to investigate the sigma-nucleus potential. The inclusive spectrum was measured at a beam momentum of 1.2 GeV/c with an energy resolution of 3.3 MeV (FWHM) by employing the superconducting kaon spectrometer system. The spectrum was compared with theoretical calculations within the framework of the distorted-wave impulse approximation, which demonstrates that a strongly repulsive sigma-nucleus potential with a nonzero size of the imaginary part reproduces the observed spectrum.

DOI: 10.1103/PhysRevLett.89.072301 PACS numbers: 21.80.+a, 13.75.Ev, 25.80.Hp, 25.80.Nv

The sigma(Σ)-nucleus potential describes the behavior of a Σ hyperon in the nuclear medium. However, the Σ-nucleus potential is still unclear because experimental information is limited, as described below. Hyperon-nucleon potentials based on a one-boson exchange model allow several sets of parameters, since hyperon-nucleon scattering data are poor. The energy shifts and widths of the Σ^--atomic x-ray transition carry information on the interaction of a Σ to a core nucleus [1,2]. The current precision of the x-ray data allows several possible potentials of various shapes inside a nucleus because the x-ray data are mainly sensitive to the potential shape outside of the nucleus. Although past measurements claimed observation of narrow peak structures in Σ-hypernuclear excitation spectra, they were excluded in later experiments [3]. The existence of a ${}^{4}_{\Sigma}$He bound state was claimed at KEK [4] and established at BNL [5]. A ${}^{4}_{\Sigma}$He bound state has been predicted theoretically [6]. The theory explains that a cancellation of the repulsive central part with the attractive isospin-dependent part (so-called Lane term) in the Σ-nucleus folding potential implies a potential shape with a repulsive core and an attractive pocket at the nuclear surface, and results in a narrow bound state. The existence of the Lane term was suggested in light nuclei, where systematic differences between the inclusive $(K^-, \pi^\pm)$ spectra were observed, although no narrow states were found [3]. Many other attempts to find narrow Σ-hypernuclear states, via the $(K^-, \pi^\pm)$ reactions on light nuclei of the mass number $A \leq 16$, have failed [7]. No data are available in heavier nuclei of $A > 16$. An analysis of the spectrum shape in the (stopped K^-, π^+) reaction on ^{12}C was made, where theoretical calculations based on the distorted-wave impulse approximation (DWIA) developed by Morimatsu and Yazaki were employed [8]. This analysis gave a limit on the real part $V_0^\Sigma > -12$ MeV and the imaginary part $W_0^\Sigma < -7$ MeV, assuming the Woods-Saxon type of the Σ-nucleus potential, expressed as $(V_0^\Sigma + iW_0^\Sigma)f(r)$, $f(r)$ being the Fermi function [9].

Recently, the role of strangeness in a neutron star has been intensively discussed. The behavior of hyperons in high-density nuclear matter determines the abundance of hyperons in a neutron star, which is related to its thermal evolution, the maximal mass of a neutron star, and a formation scenario of a neutron star or a black hole [10,11]. Σ^- is a hyperon expected to appear first in dense nuclear matter due to its negative charge [12], for which the interaction of Σ^- in nuclear matter, and hence the Σ-nucleus potential, is of particular importance. New experimental information is therefore awaited in order to improve the ambiguous situation concerning the Σ^--nucleus potential in medium heavy nuclei.

Since the Morimatsu-Yazaki formalism has been successfully applied to the analysis of the $(K^-, \pi^\pm)$ spectra in helium [13] and carbon [9], the formalism was employed for the (π^-, K^+) reaction, and the inclusive spectrum was found to be sensitive to the Σ-nucleus potential [14]. We carried out an experiment to measure the inclusive (π^-, K^+) reaction on several targets (CH_2, Si, Ni, In, and Bi) of natural isotopic composition in order to extract information on the Σ-nucleus potential [15,16]. In this

Letter, we first report on a measurement of the inclusive (π^-, K^+) spectrum on Si, and discuss the spectrum shape to derive the Σ-nucleus potential. Specifically, we obtained the information on the central part of the Σ-nucleus potential in Si since the Lane term is expected to be reduced due to its A^{-1} dependence. In heavier systems, such as In and Bi, the isospin dependence may be investigated because of their large neutron to proton ratios. We will report on the other targets elsewhere [17].

The present experiment was performed at the K6 beam line of the KEK 12-GeV Proton Synchrotron. It is known that the cross section of the elementary $p(\pi^-, K^+)\Sigma^-$ reaction decreases with an increase in the incident beam momentum at forward scattering angles. On the other hand, the momentum transfer (Δp) increases rapidly below 1.2 GeV/c. The rapid change of Δp with beam momentum complicates the spectrum analysis and a larger Δp requires a large scattered kaon acceptance. The beam momentum was thus chosen at 1.2 GeV/c. Spectroscopic studies of Λ hypernuclei have been conducted with the superconducting kaon spectrometer (SKS) system at K6. It has been demonstrated that SKS has a momentum resolution of 0.1% (FWHM) and a linearity of within 0.1 MeV/c in its momentum acceptance of $\pm 10\%$ [18]. SKS is suitable to measure the inclusive spectrum over a wide energy range. Its resolving power is helpful to maintain the sensitivity to W_0^Σ, since W_0^Σ makes the spectrum spread like a resolution function [19].

A natural Si target of 6.53 g/cm^2 was used. A CH_2 target of 1.00 g/cm^2 was placed 250 mm upstream from the Si target in tandem to monitor the energy scale, the energy resolution, and the cross section. The reaction target was identified by cutting on the reconstructed vertex position, as superimposed at the upper right corner of Fig. 1. Because a small fraction of the CH_2 contamination into the Si window was found, the measured CH_2 spectrum, properly scaled, was subtracted from the Si spectrum.

Figure 1 shows the measured missing mass spectrum on CH_2 in proton-target kinematics at a kaon scattering angle of $\theta_K = 6° \pm 2°$, where the spectrum is plotted as a function of $M_{\Sigma^-} - M_p$ (MeV/c^2). Here M_{Σ^-} and M_p represent the reconstructed missing (Σ^-) mass and the target (proton) mass, respectively. The spectrum comprises a prominent peak and a broad bump, which correspond to the proton and carbon contributions, respectively. The energy losses of a pion and a kaon in the target were taken into consideration, and the reconstructed momenta were calibrated so that the proton peak is found at the known position (259.177 $\pm$ 0.029 MeV/c^2) [20]. The detector and analysis efficiencies and the SKS acceptance were corrected to obtain the cross section. The acceptance was estimated by a Monte Carlo simulation, taking into account the detector geometry, the magnetic field distribution, and the cut conditions in the analysis.

The spectrum was fitted with two Gaussians, as plotted with the solid curve in Fig. 1. One Gaussian corresponds to the proton peak, and the other represents the carbon contribution. From the proton peak, the energy resolution was found to be 3.3 $\pm$ 0.3 MeV (FWHM). The proton-peak yield was extracted by subtracting the carbon contribution. The elementary cross sections were obtained for the other θ_K's to see the angular distribution, as shown by the closed circles in Fig. 2. The angular distribution of the $p(\pi^-, K^+)\Sigma^-$ reaction has been measured at a beam momentum of 1.225 GeV/c [21]. The crosses and the shaded area in Fig. 2 are a part of the measured points and the deduced angular distribution in the Lab frame, and compared to the previous experiment, which was originally reported in the center-of-mass frame. The shaded area shows the fitting error boundary. The present measurement agrees well with the previous one.

Figure 3 shows the inclusive (π^-, K^+) spectrum on Si as a function of the Σ^- binding energy $(-B_{\Sigma^-})$ at $\theta_K = 6° \pm 2°$. This spectrum was made by combining the data taken in three different field settings of SKS (nominal 1.9,

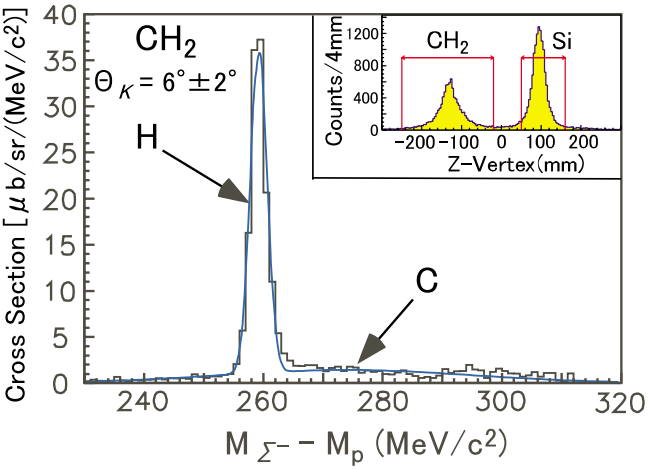

FIG. 1 (color online). Missing-mass spectrum in the proton-target kinematics of the (π^-, K^+) reaction on CH_2. The vertex distribution along the beam line is superimposed at the upper right corner. See text.

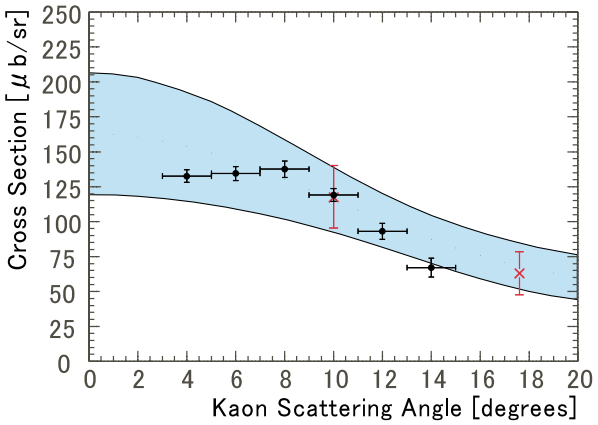

FIG. 2 (color online). Measured angular distribution (closed circles) of the elementary reaction in the Lab frame. The previous data are also shown (crosses and shaded area) [21].

2.2, and 2.4 T) in order to cover a wider kaon momentum range. The spectrum in one setting could be connected to another smoothly, since the acceptance regions partly overlap.

We found two notable features in the Si spectrum. First, the spectrum shows that the cross section gradually increases with an increase of $-B_{\Sigma^-}$. The maximum of the spectrum is achieved at $-B_{\Sigma^-} > 120$ MeV. The maximum occurs at an energy larger than that predicted by the Fermi-gas model. Second, we observed significant yields in the bound state region. These yields are beyond those expected from the combination of the Coulomb and nuclear potentials and suggest a strong Σ^--nucleus interaction.

In order to extract further information, we calculated the inclusive spectrum, according to the Morimatsu-Yazaki formalism [8]. The cross section of the inclusive reaction can be written as

$$\frac{d^2\sigma}{d\Omega dE} = \beta\left(\overline{\frac{d\sigma}{d\Omega_{el}}}\right)S(E), \tag{1}$$

where β is the kinematical factor for a coordinate transfer from a two-body system to a many-body system [22], and $\overline{d\sigma/d\Omega_{el}}$ represents the averaged differential cross section of the elementary reaction. Here the elementary cross section $[d\sigma/d\Omega(s, \Omega_K)]$ is averaged over the momentum of a proton ($\boldsymbol{k}$) moving in the target nucleus with a weight of the momentum distribution ($\rho(\boldsymbol{k})$), as written as

$$\overline{\frac{d\sigma}{d\Omega_{el}}}(E) = \frac{\int \rho(\boldsymbol{k})\frac{d\sigma}{d\Omega}(s, \Omega_K)\delta(k - P)dk}{\int \rho(\boldsymbol{k})\delta(k - P)dk}, \tag{2}$$

$$P = k_{K^+} + k_\Sigma - k_{\pi^-}. \tag{3}$$

The delta function is required for energy-momentum conservation in the elementary reaction. Relevant particles are treated on mass-shell, and the possible $\boldsymbol{k}$ is given by k_{π^-} and k_{K^+} at $E(-B_{\Sigma^-})$. As a result, $\overline{d\sigma/d\Omega_{el}}$ depends on E. In this calculation, $d\sigma/d\Omega(s, \Omega_K)$ was taken from Refs. [21,23,24], where s is the Mandelstam variable. $\rho(\boldsymbol{k})$ was given by the wave function of the initial state. The strength function ($S(E)$) is characterized by distorted waves of the incident pion and scattered kaon and the nuclear response function. The response function can be described by means of the Green's function [cf. Eq. (2.2) in Ref. [8]]. Here we assume the Woods-Saxon–type one-body potential for the Σ-nucleus potential ($U_\Sigma(r)$). The Green's function (G) is a solution of

$$[E + \hbar^2/(2\mu)\Delta - U_\Sigma(\boldsymbol{r})]G(E; \boldsymbol{r}', \boldsymbol{r}) = -\delta(\boldsymbol{r}' - \boldsymbol{r}), \tag{4}$$

where μ is the reduced mass.

Distorted waves of the pion and kaon were calculated in the eikonal approximation, employing the meson-nucleon total cross sections of $\sigma_{\pi^- N} = 35$ mb and $\sigma_{K^+ N} = 14$ mb [25]. The distortion effect reduces the magnitude of the inclusive spectrum but does not affect the spectrum shape very much. Observed (π^-, K^+) spectra on different targets show similar shapes with an increase of the magnitude as an increase of the mass number [16]. However, more careful and systematic analysis on the different targets would be needed to state the absolute strength of the distortion. The spectrum shape is directly related to the response function since the Σ-nucleus potential appears explicitly in Eq. (4). Therefore, we present the results of the shape analysis, where the measured spectrum was fitted by the calculated ones for various $U_\Sigma(r)$s. Two of the calculated spectra (solid and dashed curves) are shown in Fig. 3, for example. The potential parameters used in the calculations are listed in Table I. The solid and dashed curves are for the cases of a repulsive and a shallow Σ-nucleus potential, respectively. In the fitting, we introduced a free parameter (scaling factor) κ to adjust the magnitude of the spectrum. The scaling factor κ and χ^2 per degree of freedom (number in parentheses) are shown in Fig. 3. A shallow potential represents a weakly attractive potential, which has not been excluded by the analysis in the (stopped K^-, π^+)

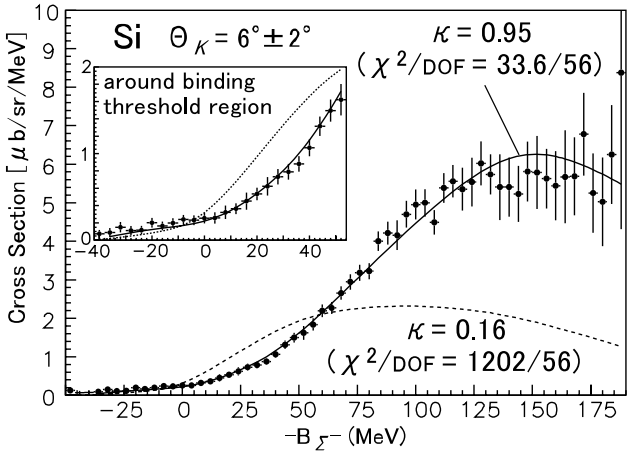

FIG. 3. Inclusive (π^-, K^+) spectrum on Si at $\theta_K = 6° \pm 2°$. The curves are the calculated spectra for the repulsive (solid) and shallow (dashed) Σ-nucleus potentials, fitted to the measured spectrum. A value of the scaling factor κ and χ^2 per degree of freedom are shown for each fitting. See text for details.

TABLE I. Potential parameters used for the present calculations. The Woods-Saxon type potential is assumed to be $U(r) = (V_0 + iW_0)f(r) + V_{SO}[\hbar/(m_\pi c)]^2 r^{-1} df/dr(\boldsymbol{\ell}\cdot\boldsymbol{\sigma}) + V_{\text{Coulomb}}(r)$, $f(r) = \{1 + \exp[(r - c)/z]\}^{-1}$.

	Σ-nucleus pot.		Initial Si
	U_Σ^{R}[a]	U_Σ^{S}[a]	U_T[b]
V_0 (MeV)	+150	-10	-49.6[d]
W_0 (MeV)	-15	-10	0
V_{SO} (MeV)	0	0	7
c (fm)	3.3[c]	3.3[c]	4.09[d]
z (fm)	0.67	0.67	0.536

[a] U_Σ^R (U_Σ^S) denotes a repulsive (shallow) Σ-nucleus potential.
[b] Proton single-particle potential of the initial nucleus (Si).
[c] $c = 1.1 \times (A - 1)^{1/3}$.
[d] These are adjusted to reproduce the proton separation energy (11.585 MeV) [26] and nuclear radius $r^{21/2} = 3.15$ fm [27].

experiment [9]. The dashed curve is greatly shifted to the lower $-B_{\Sigma^-}$ side, and does not reproduce the spectrum in shape. On the other hand, the solid curve gives the best χ^2. We made calculations for various values of the real (V_0^Σ) and imaginary (W_0^Σ) parts of the Σ-nucleus potential. It can be demonstrated that the calculated spectrum becomes lower in height and shifts toward a higher $-B_{\Sigma^-}$ in the distribution as a result of suppression in the lower $-B_{\Sigma^-}$ region along with an increase of V_0^Σ. When $|W_0^\Sigma|$ increases, the calculated spectrum becomes spread out, with a worse fitting. An increase of W_0^Σ from -10 MeV makes the fitting slightly worse, although the sensitivity becomes lower for $W_0^\Sigma \gtrsim -5$ MeV. The present fitting shows that the cases of $V_0^\Sigma \lesssim 70$ MeV give very poor χ^2s with the confidence level less than 0.1% for any W_0^Σ. In addition, the cases of $W_0^\Sigma \lesssim -30$ MeV, independent of V_0^Σ, have the confidence level less than 0.3%. Here the confidence level just represents the consistency of the model, and the above regions are far from consistency. The solid curve gives the best fitting among the variation of V_0^Σ and W_0^Σ for the present choices of the other potential parameters.

The spectrum shape depends little on the choice of the diffuseness parameter (z). The spin-orbit term $V_{\rm SO}$ in the Σ-nucleus potential may be as large as that in an ordinary nucleus. In the case of the same order of magnitude, the calculated spectrum slightly changes in the highly excited region, which does not affect the present argument. However, the spectrum is sensitive to the choice of the radius parameter (c). When c of the initial nuclear potential decreases by 10% with keeping c of the Σ-nucleus potential, the optimum V_0^Σ decreases by approximately 20%–30%, for example. In this case, the wave function of the initial state is located at the inner side of the nucleus, and thus the overlap of the initial wave to the final one becomes worse, resulting in the spectrum being pushed to a higher $-B_{\Sigma^-}$ region.

The present result shows that a strongly repulsive Σ-nucleus potential having a nonzero size of the imaginary part is required to reproduce the observed spectrum within the framework of DWIA. The repulsive Σ-nucleus potential should be taken into account for discussing the hyperon constituents of neutron stars [10]. A repulsive Σ-nucleus potential has been claimed from an analysis of the Σ^--atomic x-ray data [1,2]. Further studies on the Σ-nucleus potential, particularly for details of its shape from the central nuclear region to the outer atomic orbit region, would be required to explain the present result and the x-ray data.

The authors express their deep gratitude to Professor Y. Akaishi, Professor T. Harada, and Dr. T. Koike for invaluable discussions on the DWIA calculations. They are sincerely grateful to Dr. R. E. Chrien for the proofreading of this Letter. They thank Professor K. Nakamura, the head of Physics Division III, and Professor Y. Yoshimura of the Experiment Planning and Program Coordination Office in KEK for their support and encouragement to perform this work. The efforts of the KEK-PS staff members and the beam channel group members to deliver a stable proton beam are greatly appreciated. They are grateful to indispensable support from the Counter-Experimental Hall, Online/Electronics, and Cryogenics Groups.

*Present address: Laboratory of Physics, Osaka Electro-Communication University, Neyagawa, Osaka 572-8530, Japan.
†Present address: Brookhaven National Laboratory, Upton, New York 11973.
‡Present address: Tohoku Gakuin University, Tagajo, Miyagi 985-8537, Japan.

[1] C. J. Batty, E. Friedman, and A. Gal, Prog. Theor. Phys. Suppl. **117**, 227 (1994).
[2] J. Mareš, E. Friedman, A. Gal, and B. K. Jennings, Nucl. Phys. **A594**, 311 (1995).
[3] S. Bart *et al.*, Phys. Rev. Lett. **83**, 5238 (1999), and references therein.
[4] H. Outa *et al.*, Prog. Theor. Phys. Suppl. **117**, 177 (1994).
[5] T. Nagae *et al.*, Phys. Rev. Lett. **80**, 1605 (1998).
[6] T. Harada, S. Shinmura, Y. Akaishi, and H. Tanaka, Nucl. Phys. **A507**, 715 (1990).
[7] A review of past measurements can be found in Ref. [3].
[8] O. Morimatsu and K. Yazaki, Nucl. Phys. **A483**, 493 (1988).
[9] M. Iwasaki, Dr. thesis, University of Tokyo, 1987.
[10] S. Balberg and A. Gal, Nucl. Phys. **A625**, 435 (1997).
[11] T. Takatsuka *et al.*, Int. J. Mod. Phys. B **15**, 1609 (2001), and references therein.
[12] M. Baldo *et al.*, Phys. Rev. C **58**, 3688 (1998).
[13] T. Harada, Nucl. Phys. **A672**, 181 (2000).
[14] T. Koike *et al.* (private communication).
[15] H. Noumi *et al.*, KEK-PS Proposal No. E438.
[16] P. K. Saha, Dr. thesis, Sokendai (KEK Report No. 2001-17).
[17] P. K. Saha *et al.* (to be published).
[18] T. Fukuda *et al.*, Nucl. Instrum. Methods Phys. Res., Sect. A **361**, 485 (1995).
[19] C. B. Dover, D. J. Millener, and A. Gal, Phys. Rep. **184**, 1 (1989).
[20] D. E. Groom *et al.*, Eur. Phys. J. C **15**, 1 (2000).
[21] M. L. Good *et al.*, Phys. Rev. **183**, 1142 (1969).
[22] S. Tadokoro, H. Kobayashi, and Y. Akaishi, Phys. Rev. C **51**, 2656 (1995).
[23] J. C. Doyle *et al.*, Phys. Rev. **165**, 1483 (1968).
[24] O. I. Dahl *et al.*, Phys. Rev. **163**, 1430 (1967).
[25] C. B. Dover, L. Ludeking, and G. E. Walker, Phys. Rev. C **22**, 2073 (1980).
[26] *Table of Isotopes, Eighth Edition*, edited by R. B. Firestone *et al.* (John Wiley & Sons, New York, 1996).
[27] H. de Vries *et al.*, At. Data Nucl. Data Tables **36**, 495 (1987).